THE JOURNAL OF BIOLOGICAL CHEMISTRY VOL. 287, NO. 7, pp. 4652–4661, February 10, 2012

A High Affinity Interaction of Plasminogen with Fibrin Is Not Essential for Efficient Activation by Tissue-type Plasminogen Activator*

Received for publication, October 27, 2011, and in revised form, December 10, 2011 Published, JBC Papers in Press, December 20, 2011, DOI 10.1074/jbc.M111.317719

Paul Y. Kim[1], **Long D. Tieu, Alan R. Stafford, James C. Fredenburgh, and Jeffrey I. Weitz**[2]

From the Departments of Medicine and Biochemistry and Biomedical Sciences, McMaster University and Thrombosis and Atherosclerosis Research Institute, Hamilton, Ontario L8L 2X2, Canada

Background: Although fibrin promotes plasminogen activation by tissue-type plasminogen activator by serving as a template, the importance of the plasminogen/fibrin interaction is unclear.
Results: Fibrin promoted Lys- and Mini-plasminogen activation to a similar extent even though Mini-plasminogen bound fibrin with 117-fold lower affinity.
Conclusion: Kringle 5 of plasminogen is essential for efficient activation by the tissue-type plasminogen activator-fibrin complex.
Significance: This study identifies a novel mechanism for regulation of plasminogen activation.

Fibrin (Fn) enhances plasminogen (Pg) activation by tissue-type plasminogen activator (tPA) by serving as a template onto which Pg and tPA assemble. To explore the contribution of the Pg/Fn interaction to Fn cofactor activity, Pg variants were generated and their affinities for Fn were determined using surface plasmon resonance (SPR). Glu-Pg, Lys-Pg (des(1–77)), and Mini-Pg (lacking kringles 1–4) bound Fn with K_d values of 3.1, 0.21, and 24.5 μM, respectively, whereas Micro-Pg (lacking all kringles) did not bind. The kinetics of activation of the Pg variants by tPA were then examined in the absence or presence of Fn. Whereas Fn had no effect on Micro-Pg activation, the catalytic efficiencies of Glu-Pg, Lys-Pg, and Mini-Pg activation in the presence of Fn were 300- to 600-fold higher than in its absence. The retention of Fn cofactor activity with Mini-Pg, which has low affinity for Fn, suggests that Mini-Pg binds the tPA-Fn complex more tightly than tPA alone. To explore this possibility, SPR was used to examine the interaction of Mini-Pg with Fn in the absence or presence of tPA. There was 50% more Mini-Pg binding to Fn in the presence of tPA than in its absence, suggesting that formation of the tPA-Fn complex exposes a cryptic site that binds Mini-Pg. Thus, our data (*a*) indicate that high affinity binding of Pg to Fn is not essential for Fn cofactor activity, and (*b*) suggest that kringle 5 localizes and stabilizes Pg within the tPA-Fn complex and contributes to its efficient activation.

Fibrinolysis, the process that degrades fibrin (Fn)[3] clots, is initiated when tissue-type plasminogen activator (tPA) converts the zymogen plasminogen (Pg) to plasmin (Pn), the enzyme that solubilizes Fn (1, 2). A distinguishing feature of tPA is its affinity for Fn. By serving as a template onto which both tPA and Pg bind, Fn promotes enzyme-substrate interaction through formation of a ternary complex. Consequently, the catalytic efficiency of Pg activation by tPA is 3 orders of magnitude greater in the presence of Fn than it is in its absence and 2 orders of magnitude greater in the presence of fibrinogen (Fg), the soluble precursor of Fn (3–5). These features render tPA Fn-specific; enhanced Pn generation on the Fn surface promotes clot dissolution, whereas inefficient Pg activation in the presence of Fg limits systemic Fg degradation. Urokinase-type plasminogen activator (uPA), in contrast to tPA, does not bind to Fn (2). Consequently, the catalytic efficiency of Pg activation by uPA in the presence of Fn is similar to that in its absence, or in the presence of Fg. Because Pn generation is not localized to the Fn surface, uPA lacks Fn specificity. The functional differences between tPA and uPA identify Fn affinity as a critical determinant of Fn specificity. Thus, the capacity of Fn to promote Pg activation on its surface is dependent on the Pg activator/Fn interaction.

In contrast to the role played by the activator/Fn interaction, the contribution of the Pg/Fn interaction to the potentiating effect of Fn is unclear. The predominant form of Pg, termed Glu-Pg, is a single-chain glycoprotein consisting of an NH_2-terminal peptide, five kringle domains, and a protease domain (6, 7). Lys-Pg, a truncated Pn-derived form that lacks the NH_2-terminal 1–77 peptide is produced during fibrinolysis (Fig. 1*A*) (8). Whereas Glu-Pg assumes a closed conformation because of intramolecular links between the NH_2-terminal peptide and

* The work was supported in part by Canadian Institutes of Health Research Grants MOP 3992, MOP 102735, and CTP 79846, the Heart and Stroke Foundation of Ontario, and the Ontario Research and Development Challenge Fund.

This publication is dedicated to the memory of Dr. Michael E. Nesheim, a pioneer in thrombosis research, and a dear friend to all of us. He will be greatly missed.

[1] Recipient of a Research Fellowship Award from the Heart and Stroke Foundation of Canada and AstraZeneca Canada.

[2] Canada Research Chair (Tier 1) in Thrombosis and the Heart and Stroke Foundation of Ontario/J. Fraser Mustard Chair in Cardiovascular Research. To whom correspondence should be addressed: 237 Barton St. East, Hamilton, Ontario L8L 2X2, Canada. Tel.: 905-574-8550; Fax: 905-575-2646; E-mail: weitzj@taari.ca.

[3] The abbreviations used are: Fn, fibrin; Pg, plasminogen; Pn, plasmin; Fg, fibrinogen; tPA, tissue-type plasminogen activator; uPA, urokinase-type plasminogen activator; SPR, surface plasmon resonance; RU, response units; VFKck, Val-Phe-Lys-chloromethyl ketone; FPRck, Phe-Pro-Arg-chloromethyl ketone; ϵ-ACA, ϵ-amino-*n*-caproic acid.

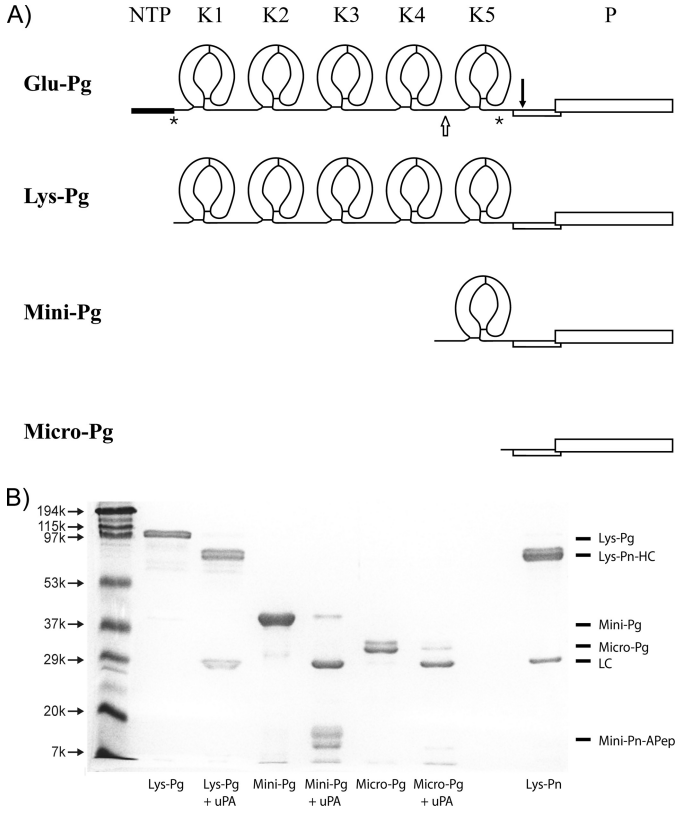

FIGURE 1. **Plasminogen variants.** *A*, secondary structures of Pg variants displaying the kringle and protease domains of Glu-, Lys-, Mini-, and Micro-Pg. The *asterisks* (*) represent Pn cleavage sites between Lys-77 and Lys-78 (8, 30) and between Arg-530 and Lys-531 (31). The *open arrow* represents the elastase cleavage site between Val-441 and Val-442 (16). The *solid inverted arrow* indicates the tPA or uPA cleavage site between Arg-561 and Val-562 (1, 32, 33). *NTP*, NH_2-terminal peptide; *K1* through *K5*, kringle domains 1 through 5; *P*, protease domain. *B,* SDS-PAGE analysis of the isolated Pg variants under reducing conditions before and after uPA treatment to convert them to their respective Pn forms. Molecular weight markers are labeled on the *left*. *Pn*, obtained by uPA activation of Glu-Pg, was included as a control. The identities of the protein bands are labeled on the right. *Lys-Pn-HC*, Lys-Pn heavy chain; *LC*, light chain; *Mini-Pn-Apep*, Mini-Pn activation peptide.

kringle 5 domains, Lys-Pg has a more open conformation. The conformational change that occurs upon conversion of Glu-Pg to Lys-Pg not only renders Lys-Pg more readily activated by Pg activators, but also endows Lys-Pg with higher affinity for Fn than its intact precursor. Of the five kringle domains in Pg, kringles 1, 4, and 5 are reported to be the major mediators of the Pg/Fn interaction (9, 10).

To refine our understanding of the role of Fn as a cofactor, Pg activation was quantified using Pg and activator forms possessing different affinities for Fn. Using four Pg derivatives, we compared their (*a*) affinities for immobilized Fn or Fg using surface plasmon resonance (SPR), and (*b*) kinetics of activation by tPA or uPA in the absence of a cofactor with those in the presence of Fn or Fg. We also used SPR to compare the affinities of the various Pg derivatives for tPA because the binary Pg/tPA interaction may influence the kinetics of activation when the affinity of Pg for Fn decreases. We hypothesized that if the Pg/Fn interaction is an important determinant of the capacity of Fn to promote Pg activation by tPA, Fn cofactor activity would be attenuated or eliminated with Mini- and Micro-Pg, respectively, which exhibit little or no affinity for Fn. In contrast, because uPA does not bind to Fn, we postulated that Fn would have little or no effect on the kinetics of activation of all four forms of Pg by uPA.

EXPERIMENTAL PROCEDURES

Materials—H-D-Val-Leu-Lys-*p*-nitroaniline-dihydrochloride (S2251) was from Chromogenix (Milan, Italy), whereas benzamidine-Sepharose was from Amersham Biosciences. Streptavidin-agarose, Tween 80, Tween 20, and human serum albumin were obtained from Sigma. Precast 4–15% SDS-polyacrylamide gels were from Bio-Rad. Human neutrophil elastase was purchased from Elastin Products Co. (Owensville, MO). Human thrombin was purchased from Enzyme Research Laboratories (South Bend, IN). Val-Phe-Lys-chloromethyl ketone (VFKck) and Phe-Pro-Arg-chloromethyl ketone (FPRck) were purchased from EMD Chemicals (Gibbstown, NJ). Biotinylated FPRck (biotin-FPRck) was obtained from Hematologic Technologies Inc. (Essex Junction, VT). Recombinant tPA (Activase) was kindly provided by Dr. B. Keyt (Genentech, South San Francisco, CA), whereas uPA was purchased from Calbiochem. Fg was prepared using the procedure of Straughn and Wagner (11) with the modifications described by Walker and Nesheim (12), except that the first PEG-8000 cut was performed at 1.2%, which increased the final yield of Fg to ~0.4 mg/ml of starting plasma. Isolated Fg was stored at −80 °C. The integrity of all purified proteins was confirmed by SDS-PAGE analysis, and concentrations were determined by photospectrometry.

Isolation of Glu-, Lys-, Mini-, and Micro-Pg—Native Glu-Pg was isolated from citrated fresh frozen human plasma by lysine-Sepharose (Lys-Sepharose) affinity chromatography using the method of Castellino and Powell (13) and the modifications described by Stewart *et al.* (14). Pn was generated by incubating 24 μM Glu-Pg in 0.02 M Tris-HCl, 0.15 M NaCl, pH 7.4 (TBS), with 48 nM uPA for 60 min at 25 °C with constant mixing, prior to addition of another 48 nM uPA and a further 60 min incubation. The extent of Pn generation was determined by monitoring the rate of S2251 hydrolysis. Once a maximal rate was achieved, the mixture was loaded onto a 2.5 × 20-cm Lys-Sepharose column prewashed and equilibrated with TBS. After washing with TBS to remove uPA, Pn was eluted with TBS containing 20 mM ϵ-ACA (14). Protein-containing fractions were pooled, dialyzed against TBS, concentrated, and stored in aliquots at −80 °C. Concentration was determined by photospectrometry.

Lys-Pg was generated by Pn hydrolysis of Glu-Pg as described previously by Nesheim *et al.* (15) with the modifications of Stewart *et al.* (14). Briefly, Glu-Pg (10 μM) was converted to Lys-Pg by incubation for 2 h at 25 °C with 0.16 μM Pn in 0.02 M HEPES, 0.15 M NaCl, pH 7.4 (HBS), and 0.01% Tween 80 (HBST) containing 50 mM ϵ-ACA. Additional Pn (0.16 μM) was added and the mixture was incubated for another 2 h. To remove Pn, a 10-fold molar excess of biotin-FPRck was added and incubated for 2 h at 25 °C while monitoring aliquots for Pn activity by S2251 hydrolysis. When no Pn activity was detected, the mixture was dialyzed against 4 × 1 liter of HBST prior to addition of streptavidin-agarose suspended in HBST. After centrifugation, the solution was filtered to remove any traces of streptavidin-agarose, and after confirming the absence of resid-

ual biotin-FPRck by showing no reduction in Pn-mediated S2251 hydrolysis, the solution was stored in aliquots at −80 °C. Concentration was determined by photospectrometry.

Mini-Pg was generated as described previously (16) with some modifications. Briefly, after incubating 33 μM Glu-Pg with 0.67 μM elastase in TBS for 60 min at 25 °C, the reaction was terminated by adding 2 mM phenylmethylsulfonyl fluoride. The mixture was dialyzed against 0.1 M sodium phosphate, pH 8.0 (NaP_i), for 2 h at 4 °C, and then loaded onto a Lys-Sepharose column pre-equilibrated with NaP_i. After washing with the same buffer, the flow-through, which only contained Mini-Pg, was collected and protein-containing fractions were pooled, dialyzed against TBS, and concentrated by centrifugation. Concentration was determined by photospectrometry using an extinction coefficient of 16.0 ($\epsilon^{1\,cm}_{1\%}$ (280 nm)) and molecular mass of 38,000 Da, as reported previously (16). Mini-Pg was then stored in aliquots at −80 °C.

Micro-Pg was prepared as described previously (17) with modifications. Briefly, 190 μM Glu-Pg was incubated with 3 μM uPA-free Pn for 48 h at 25 °C with constant mixing. The mixture was then applied to a Lys-Sepharose column pre-equilibrated with NaP_i. After washing with the same buffer, protein-containing fractions were pooled and traces of Pn, detected by monitoring S2251 hydrolysis, were removed by loading the mixture onto a benzamidine-Sepharose column that was pre-washed and equilibrated with NaP_i. Pn-free, protein-containing fractions were pooled, dialyzed against TBS, and concentrated by centrifugation. Concentration was determined by photospectrometry using an extinction coefficient of 16.0 ($\epsilon^{1\,cm}_{1\%}$ (280 nm)) and molecular mass of 28,617 Da (17), Micro-Pg was stored in aliquots at −80 °C.

The integrity of Lys-, Mini-, and Micro-Pg was assessed by SDS-PAGE under reducing conditions (Fig. 1*B*). Each form displayed the expected molecular weight and was activable by uPA.

Affinities of Pg Variants for Fg or Fn—Binding interactions were studied by SPR using a Biacore 1000 (Piscataway, NJ). Fg and albumin were biotinylated by coupling to a biotin-EZ-Link spacer consisting of sulfosuccinimidyl-6-(biotinamido)hexanoate (Thermo Fisher Scientific Inc., Rockford, IL). Biotinylated Fg or albumin in HBS containing 2 mM $CaCl_2$ and 0.005% Tween 20 (HBSC-Tween 20) was then adsorbed to a streptavidin-coated (SA) sensor chip (Biacore) at a flow rate of 5 μl/min until 5000 response units (RU) of Fg or 4000 RU of albumin were immobilized.

For studies with Fn, immobilized Fg was converted to Fn by injecting 0.5 μM thrombin in HBSC-Tween 20 at a rate of 10 μl/min for 30 min as described previously (18, 19). This procedure was repeated at least twice and was continued until there was no further reduction in RU, indicating complete conversion of Fg to Fn. Flow cells were then washed with 0.02 M HEPES, 1 M NaCl, 2 mM $CaCl_2$, pH 7.4, containing 0.005% Tween 20 and equilibrated with HBSC-Tween 20.

Binding studies were performed with a range of Glu- (0–20 μM), Lys- (0–0.75 μM), Mini- (0–20 μM), or Micro-Pg (0–20 μM) concentrations diluted in HBSC-Tween 20 containing a 2-fold molar excess of VFKck. Samples were injected at a rate of 20 μl/min for 2 min and the cells were then washed with HBSC-Tween 20 to monitor dissociation. Between runs, the cells were regenerated with 0.02 M HEPES, 1 M NaCl, pH 7.4, containing 20 mM ϵ-ACA. The binding data were analyzed using the steady-state affinity model (Biacore). In the sensorgrams where RU values approached a plateau, RU bound was determined by subtracting the control RU values obtained in the albumin channel from those obtained with Fg or Fn. Corrected RU values were then plotted against the starting concentrations of Pg, and data were fit to a rectangular hyperbola to determine K_d values using SigmaPlot (version 8, SPSS).

Similar studies were performed in the presence of active site-blocked tPA (FPR-tPA), which was generated by incubating 1 mg/ml of tPA with a 20-fold molar excess of FPRck for 2 h, followed by dialysis against HBS. Analytes, which contained 25 nM FPR-tPA and the various Pg derivatives in a range of concentrations were co-injected into flow cells containing immobilized biotinylated Fn. Pg binding to Fn in the presence of tPA was corrected for tPA binding to Fn alone. The total RU change at saturation was then plotted against the starting concentration of Pg and the K_d was determined by nonlinear regression as described above.

Binding of Pg Variants to tPA—Binding interactions were studied using SPR. tPA was inactivated by incubation with biotin-FPRck. Biotin-FPR-tPA, dissolved in HBSC-Tween 20, was then adsorbed to a SA sensor chip at a flow rate of 5 μl/min to an RU of 1800. Binding studies were carried out with Glu-, Lys-, Mini-, or Micro-Pg, in concentrations up to 20 μM, diluted in HBSC-Tween 20 containing a 2-fold molar excess of VFKck relative to Pg. Samples were injected at a rate of 20 μl/min for 2 min and flow cells were then washed with HBSC-Tween 20 to monitor dissociation. Between injections, the flow cells were regenerated with 0.02 M HEPES, 1 M NaCl, pH 7.4, containing 20 mM ϵ-ACA. To normalize RU values, the RU change at saturation with each Pg variant was then divided by its molecular mass and the normalized values were then plotted against the starting concentration of Pg.

Kinetics of Activation of Pg Derivatives by tPA or uPA in Absence or Presence of Fg or Fn—Microtiter plates were pretreated for at least 1 h with HBS containing 1% Tween 80 and washed thoroughly with water. For studies with Fg, Glu-Pg (0–18 μM), Lys-Pg (0–5 μM), Mini-Pg (0–18 μM), or Micro-Pg (0–6.5 μM) was incubated at 37 °C with 5 mM $CaCl_2$ and 400 μM S2251 in the absence or presence of 1 μM Fg in HBST. Reactions were initiated by addition of tPA or uPA, and absorbance was monitored at 405 and 450 nm using a SpectraMax Plus microplate reader (Molecular Devices, Sunnyvale, CA). A tPA concentration of 0.25 nM was used with all Pg derivatives; in contrast, 1 nM uPA was used with Glu-, Lys-, and Micro-Pg, whereas 0.5 nM uPA was used with Mini-Pg.

For studies with Fn, Glu-Pg (0–0.7 μM), Lys-Pg (0–0.05 μM), Mini-Pg (0–0.7 μM), or Micro-Pg (0–6.5 μM) was incubated at 37 °C with 5 mM $CaCl_2$ and 400 μM S2251 in the absence or presence of 1 μM Fg in HBST. Reactions were initiated by the addition of 10 nM thrombin and either tPA or uPA, in the same concentrations used for the studies with Fg, and absorbance was then monitored at 405 and 450 nm. Absorbance at 405 nm was corrected for turbidity by subtracting absorbance determined at 450 nm. The rate of Pn generation (r) was determined

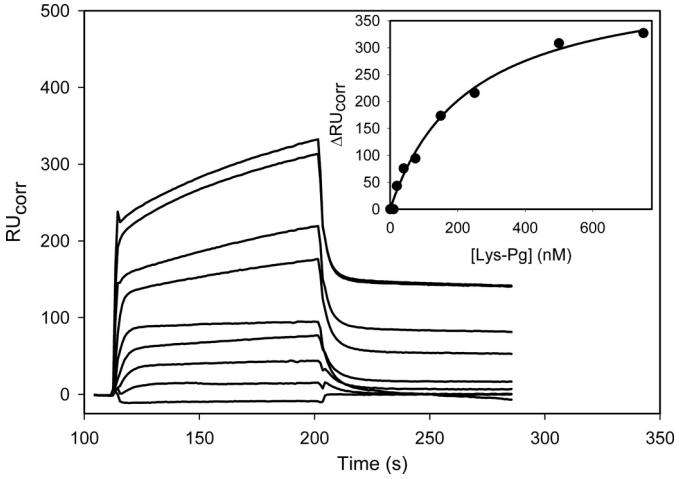

FIGURE 2. **SPR analysis of the interaction of the Lys-Pg with immobilized Fn.** Lys-Pg, at varying concentrations (0, 10, 20, 40, 75, 150, 250, 500, and 750 nM), was injected into a flow cell containing immobilized Fn or albumin for ~120 s prior to washing with HBSC-Tween 20. The *inset* illustrates the change in RU_{corr}, obtained by subtraction of the nonspecific binding to albumin, as a function of the Lys-Pg concentration. The data were then fit to a single rectangular hyperbola equation to determine the K_d value of 225.5 nM (*line*).

as described previously (20). Using the relationship $A_{corr} = (SA \times r/2) \times t^2$, corrected absorbance values (A_{corr}) were plotted against t^2 to determine the slope ($SA \times r/2$), where SA is the specific activity of Pn against S2251, r is the rate of Pn generation, and t is time. The rate was then calculated using the SA, which was experimentally determined to be 1.439 A_{corr}/min/μM. Rates were then plotted against the starting concentrations of the Pg derivatives and the data were fit to the Michaelis-Menten equation by nonlinear regression using SigmaPlot to determine the individual k_{cat} and K_m values. For reactions displaying linear rate *versus* substrate relationships, the slope of the line was taken as the catalytic efficiency. Because there is substantial change in turbidity when Fn polymerizes, more rigorous correction was necessary to accurately quantify the rate of Pn generation, as described by Schneider and Nesheim (21). The correction factor was determined experimentally by forming Fn clots in the absence of added tPA or uPA. Absorbance at 405 nm, which reflects turbidity, was 1.7-fold higher than absorbance readings at 450 nm. Therefore, turbidity readings at 450 nm were multiplied by this correction factor prior to subtraction from the 405 nm readings ($A_{corr} = A_{405} - (1.7 \times A_{450})$) to obtain those readings that solely reflect S2251 hydrolysis. Corrected absorbance values were again plotted against time squared and activation rates were determined as described above. The specific activity of Pn against S2251 in a 1 μM Fn clot was 0.924 A_{corr}/min/μM.

RESULTS

Affinities of Various Pg Variants for Fg or Fn—Affinities of the Pg variants for immobilized Fg or Fn were assessed by SPR. The binding of Lys-Pg to Fn is illustrated in Fig. 2; RU values increased with increasing Lys-Pg concentration. The changes in corrected RU values were plotted against the corresponding concentration of Lys-Pg (Fig. 2, *inset*) and the K_d value was determined by nonlinear regression analysis. A similar approach was taken to determine the K_d values for Glu-, Lys-, and Mini-Pg binding to Fg or Fn. With Micro-Pg, the signal change did not approach saturation, even with concentrations up to 20 μM, indicating a lower limit to the K_d value. Binding data are summarized in Table 1.

TABLE 1

K_d values for the interaction of the Pg variants with Fg or Fn as determined using SPR

Values represent the mean ± S.D., as determined in at least 3 separate experiments.

	Fg	Fn
	μM	
Glu-Pg	12.5 ± 2.9	3.1 ± 0.3
Lys-Pg	0.25 ± 0.03	0.21 ± 0.03
Mini-Pg	10.5 ± 2	24.5 ± 5.8
Micro-Pg	>20	>20

The affinity of Glu-Pg for Fn was 4-fold higher than that for Fg; K_d values were 3.1 and 12.5 μM, respectively. In previous reports, the affinity of Glu-Pg for Fn ranged from 13 to 38 μM and there was low or no measurable affinity of Glu-Pg for Fg (14, 22). Therefore, the higher affinity of Glu-Pg for Fn relative to Fg is consistent with previous work, which validates the use of SPR for determination of the affinity for Fg and Fn, as observed previously with thrombin (18, 19). Compared with Glu-Pg, Lys-Pg bound Fg and Fn with 50- and 15-fold higher affinities, respectively; K_d values were 0.25 and 0.21 μM, respectively. As expected, with the loss of lysine-binding kringle domains, Mini-Pg bound Fg and Fn with low affinity; K_d values were 10.5 and 24.5 μM, respectively. This represents an 8-fold decrease in Fn affinity compared with Glu-Pg and a 117-fold decrease compared with Lys-Pg. Micro-Pg, which does not possess any kringle domains, exhibited minimal binding to both Fg or Fn, consistent with previous reports that kringles 1, 4, and 5 mediate the interaction of Pg with Fg or Fn (9, 23, 24).

Affinities of Various Pg Variants for tPA—The Pg/tPA interaction was studied using SPR to explore the influence of this binary interaction on Pg activation. Because changes in RU are directly proportional to the molecular mass of the ligand, the observed RU values were first corrected for the molecular mass of the Pg variant used, and then plotted against the initial Pg concentration (Fig. 3). Pg variants bound to biotin-FPR-tPA, albeit with low affinity. Glu-Pg had the lowest affinity; an interaction that was immeasurable experimentally. In contrast, variants with an open conformation bound with higher affinities. All interactions were lysine-dependent because they were eliminated when ϵ-ACA was co-injected (data not shown). Lys-Pg, Mini-Pg, and Micro-Pg bound tPA with estimated K_d values of 3.4, 85, and 1.6 μM, respectively. Considering the ϵ-ACA sensitivity, our data raise the possibility that the protease domain of Pg interacts with the kringle 2 domain of tPA because the K_d of Micro-Pg for tPA reported here is almost identical to the K_d value for the kringle-dependent interaction of tPA with Fn (4).

Kinetics of Glu-, Lys-, Mini-, or Micro-Pg Activation by tPA or uPA—To complement the binding studies, the rates of tPA-mediated Pg activation were measured in the absence or presence of Fn or Fg. Rates of Pn formation were plotted against the starting concentration of Pg (Fig. 4), and individual k_{cat} and K_m values were determined by nonlinear regression analysis using the Michaelis-Menten equation (Table 2). Glu-, Lys-, and Mini-Pg activation by tPA in the presence of Fn are illustrated

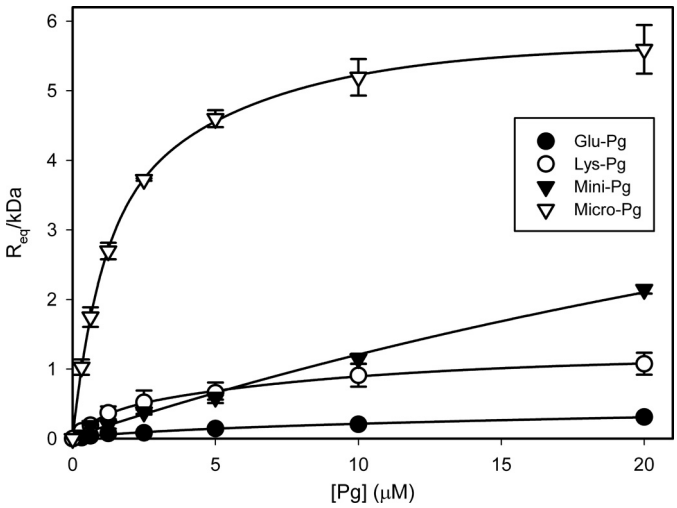

FIGURE 3. **SPR analysis of the interaction of Pg variants with tPA.** Glu- (*closed circles*), Lys- (*open circles*), Mini- (*closed triangles*), or Micro-Pg (*open triangles*), at varying concentrations (0–20 μM), were injected into a SA chip flow cell containing immobilized biotin-FPR-tPA. RU values at equilibrium binding (R_{eq}) were normalized for the molecular mass of each Pg variant and plotted against initial Pg concentrations. The data were then fit to a single rectangular hyperbola equation (*lines*). The K_d values of each Pg variant were calculated using the estimated individual on and off rates. The *error bars* indicate S.D. of at least three separate experiments.

in Fig. 4. Using these values, catalytic efficiencies (k_{cat}/K_m) were calculated (Table 3). Activation experiments were repeated in the presence of Fg. The catalytic efficiencies were estimated from the slopes of the initial linear portions of the rate *versus* Pg concentration plots because the rates did not reach a plateau (Table 2). Micro-Pg activation did not reach a plateau in any of the cofactor conditions (Fig. 4*D*), and thus only the catalytic efficiency values were reported (Table 4).

The catalytic efficiency values for each Pg variant were compared in two ways. First, we calculated cofactor ratios by dividing the catalytic efficiency of tPA-mediated activation of each Pg derivative determined in the presence of Fg or Fn by that determined in their absence (Table 3). The cofactor ratios for Fg ranged from 6 to 19 for Glu-, Lys-, and Mini-Pg. These values are consistent with the modest stimulatory activity of Fg as a cofactor (5). As expected, the catalytic efficiencies with Fn were at least an order of magnitude higher; thus, cofactor ratios range from 295 to 608, except with Micro-Pg where the cofactor ratios were 1 and 5 with Fg and Fn, respectively. These findings reveal that, despite a 100-fold difference in affinity of the different forms of Pg for Fn, the cofactor activity of Fn is constant, suggesting that cofactor activity is predominantly expressed through tPA.

Second, Pg ratios were calculated based on the ratio of catalytic efficiency of each Pg variant relative to that of Glu-Pg with Fg or Fn (Table 3). The Pg ratio for Lys-Pg was ~20, regardless of cofactor. This is consistent with previous observations that Lys-Pg is a better substrate for tPA than Glu-Pg, a phenomenon attributed to the more open conformation of Lys-Pg (5). Mini-Pg also demonstrated an order of magnitude greater Pg ratio regardless of cofactor. The Pg ratio for Micro-Pg decreased when Fg or Fn was present, suggesting that any catalytic advantage of its conformation was lost when cofactor is present.

Analysis of k_{cat} and K_m values (Table 2) reveals that the 18-fold increase in catalytic efficiency of Lys-Pg activation relative to Glu-Pg in the presence of Fn predominantly reflects a decrease in K_m, a finding in agreement with previous reports (4, 5). The decrease in K_m is consistent with the fact that Lys-Pg binds Fn with 15-fold higher affinity than Glu-Pg (Table 1). Based on these observations, the catalytic efficiency of Mini-Pg activation by tPA in the presence of Fn would be expected to be lower than that of Glu- or Lys-Pg because Mini-Pg binds Fn with an affinity 8- and 117-fold lower than those of Glu- and Lys-Pg, respectively (Table 1). However, the catalytic efficiency of Mini-Pg activation by tPA in the presence of Fn is 9-fold higher than that of Glu-Pg, resulting from a 3-fold increase in k_{cat} and 3-fold reduction in K_m. These data suggest that Mini-Pg is a good substrate for the tPA-Fn complex even though it lacks measurable affinity for fibrin. Individual kinetic parameters for Micro-Pg could not be determined because saturation was not achieved (Fig. 4).

Interestingly, in the absence of a cofactor, Lys- (Fig. 4*B*, *inset*), Mini- (Fig. 4*C*, *inset*), and Micro-Pg (Fig. 4*D*) exhibit similar ~18-fold enhancements in catalytic efficiencies compared with Glu-Pg (Fig. 4*A*, *inset*) (Table 2). This finding raises the possibility that the protease domain of Pg, the only domain common to all three forms of Pg, interacts directly with tPA.

To examine the contribution of the interaction of the Pg activator with Fg or Fn to cofactor activity, we used uPA instead of tPA because uPA does not bind Fg or Fn (2). With uPA, the catalytic efficiency values for each form of Pg in the absence of a cofactor were an order of magnitude higher than those with tPA. Also, as expected, the Pg ratios demonstrate that Lys-, Mini-, and Micro-Pg are better substrates for uPA than Glu-Pg. However, a striking divergence is noted with the cofactor ratios. The cofactor ratios with all forms of Pg were ~1 (Table 4), indicating that Fg and Fn have little effect on the catalytic efficiency of Pg activation by uPA. The lack of cofactor activity is consistent with the fact that uPA does not bind to Fg or Fn and supports the concept that the interaction of the substrate with the cofactor is a minor contributor to cofactor activity.

Influence of Fn on Pg/tPA Interaction—Despite its low affinity for Fn (Table 1), the catalytic efficiency of Mini-Pg activation by tPA is almost 9-fold higher in the presence of Fn than in its absence, raising the possibility that on the Fn surface, there is a direct Pg/tPA interaction that is distinct from the binary Pg/Fn and Pg/tPA interactions. To explore this possibility, we used SPR to examine whether the interaction of the Pg variants with Fn was altered in the presence of FPR-tPA. Pg variants were injected into flow cells containing immobilized Fn in the absence or presence of FPR-tPA. Co-injection of FPR-tPA had little effect on the binding of Glu-Pg, Lys-Pg, or Micro-Pg to Fn (data not shown). In contrast, with Mini-Pg, co-injection with FPR-tPA altered the binding profile (Fig. 5). The K_d values for the interaction of Mini-Pg with Fn in the absence or presence of FPR-tPA were calculated using individual on- and off-rates by fitting either a single- or a two-site model to the sensorgram data. In the absence of tPA (Fig. 5*A*), Mini-Pg bound Fn with a profile that best fit a single binding site model with a χ^2 value of 3.2% of the R_{max}, which is indicative of a good fit (25). Fitting to a one-site model yielded a K_d value of 31.3 μM, a value similar to

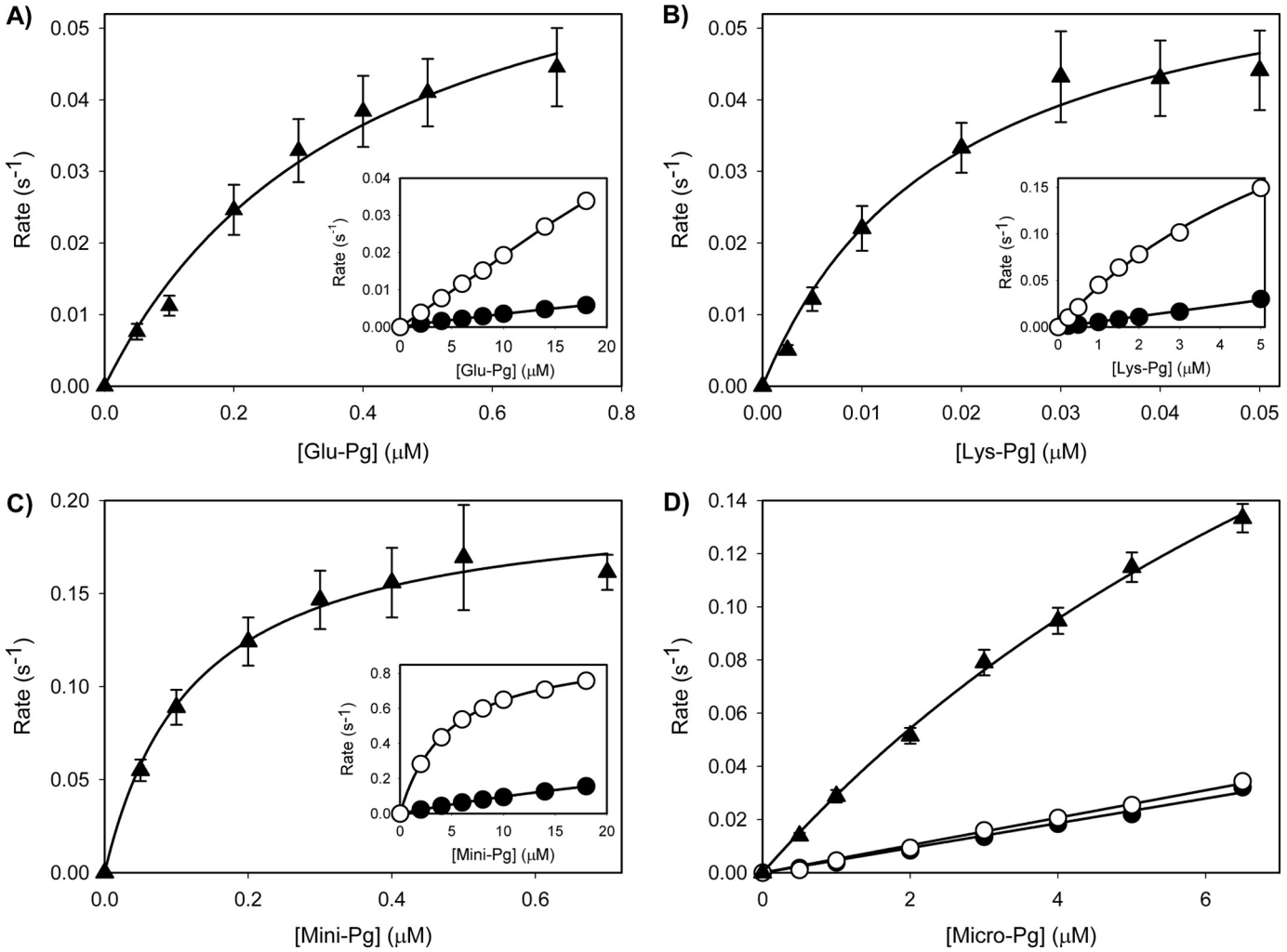

FIGURE 4. **Kinetic analyses of the activation of the Pg variants by tPA in the absence or presence of Fg or Fn.** (*A*) Glu-Pg, (*B*) Lys-Pg, (*C*) Mini-Pg, or (*D*) Micro-Pg, at varying concentrations in HBST containing 5 mM $CaCl_2$ and 400 μM S2251, were activated by the addition of 0.25 nM tPA in the absence (*closed* circles) or presence of 1 μM Fg (*open circles*). For studies with Fn (*triangles*), similar experiments were conducted except 1 μM Fg was converted to Fn by addition of 10 nM thrombin. Turbidity was monitored at 405 and 450 nm using a microtiter plate reader, and absorbance values at 405 nm were corrected for turbidity determined at 450 nm as described under "Experimental Procedures." Corrected rates of Pn generation were then plotted *versus* initial Pg concentrations and the catalytic efficiency values were determined by nonlinear regression analyses of the Michaelis-Menten equation (*lines*). The *error bars* indicate S.D. of at least three separate experiments.

TABLE 2

Turnover number (k_{cat}) and Michaelis constant (K_m) values for the activation of the various Pg derivatives by tPA in the presence of Fn

Values represent the mean ± S.D. of at least 3 separate experiments.

	k_{cat}	K_m
	s^{-1}	μM
Glu-Pg	0.073 ± 0.017	0.41 ± 0.03
Lys-Pg	0.064 ± 0.016	0.02 ± 0.001
Mini-Pg	0.220 ± 0.057	0.14 ± 0.004

the observed K_d of Mini-Pg for Fn using the steady-state affinity method (Table 1). In the presence of FPR-tPA (Fig. 5*B*), however, the sensorgram with each Mini-Pg concentration exhibited an additional slow-binding phase, suggesting two binding sites. As expected, the binding data exhibited a better fit to a two-site model than to a single-site model (χ^2 values 2.6 and 14.5% of R_{max}, respectively) with K_d values of 35.8 and 131 μM for the high and low affinity sites, respectively. Additionally, the initial fast binding appears to approach a plateau similar to the

TABLE 3

Catalytic efficiency values for the activation of the Pg variants by tPA in the absence or presence of Fg or Fn

Cofactor ratios were calculated by dividing the catalytic efficiency determined in the presence of Fg or Fn by that determined in their absence. Pg ratios were calculated by dividing the catalytic efficiency of activation of each Pg variant by that determined with Glu-Pg under the same cofactor condition. Values represent the mean ± S.D. of at least 3 separate experiments.

	Cofactor	Catalytic efficiency	Cofactor ratio	Pg ratio
		$(\times 10^{-4})\ M^{-1}\ s^{-1}$		
Glu-Pg	None	0.03 ± 0.003	1.0	1.0
	Fg	0.19 ± 0.006	6.3	1.0
	Fn	18.25 ± 5.03	608.3	1.0
Lys-Pg	None	0.60 ± 0.04	1.0	20.0
	Fg	4.91 ± 0.38	8.2	25.8
	Fn	336.24 ± 84.30	560.4	18.4
Mini-Pg	None	0.54 ± 0.18	1.0	18.0
	Fg	10.21 ± 1.22	18.9	53.7
	Fn	159.16 ± 39.48	294.7	8.7
Micro-Pg	None	0.52 ± 0.09	1.0	17.3
	Fg	0.54 ± 0.04	1.0	2.8
	Fn	2.81 ± 0.67	5.4	0.2

TABLE 4

Catalytic efficiency values for the activation of the Pg variants by uPA in the absence or presence of Fg or Fn

Cofactor and Pg ratios were calculated as described in Table 3. Values represent the mean ± S.D. of at least 3 separate experiments.

	Cofactor	Catalytic efficiency	Cofactor ratio	Pg ratio
		$(\times 10^{-4})_M{}^{-1}\,s^{-1}$		
Glu-Pg	None	1.48 ± 0.72	1.0	1.0
	Fg	0.77 ± 0.30	0.5	1.0
	Fn	0.57 ± 0.20	0.4	1.0
Lys-Pg	None	14.85 ± 0.47	1.0	10.0
	Fg	10.24 ± 0.14	0.7	13.3
	Fn	7.54 ± 0.54	0.5	13.2
Mini-Pg	None	10.61 ± 0.58	1.0	7.2
	Fg	13.33 ± 1.46	1.3	17.3
	Fn	10.96 ± 0.68	1.0	19.2
Micro-Pg	None	6.06 ± 0.49	1.0	4.1
	Fg	3.63 ± 0.36	0.6	4.7
	Fn	4.02 ± 0.77	0.7	7.1

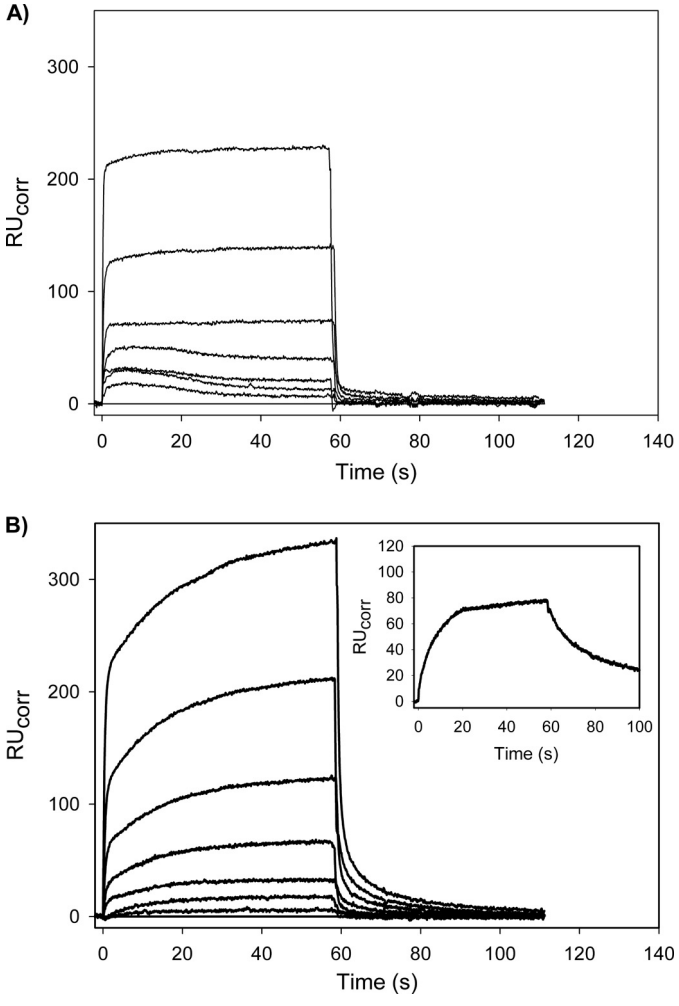

FIGURE 5. **SPR analysis of the interaction of Mini-Pg with Fn in the absence or presence of FPR-tPA.** Mini-Pg, at varying concentrations (0, 0.31, 0.63, 1.25, 2.5, 5, 10, and 20 μM), was injected for about 60 s into a SA chip flow cell containing immobilized biotin-Fn in the absence (*A*) or presence (*B*) of 25 nM FPR-tPA to measure association. Cells were then washed with HBSC-Tween 20 to monitor dissociation. Between injections, the flow cell was regenerated with 1 M NaCl containing 20 mM ϵ-ACA in HBSC-Tween 20. In the absence of tPA (*panel A*), the K_d value determined was 31.3 μM. With FPR-tPA co-injection (*panel B*), K_d values for the high and low affinity binding sites determined using a two-site model were 35.8 and 131 μM, respectively. The *inset* in *panel B* displays the slow association and dissociation of the interaction of 25 nM FPR-tPA with immobilized Fn.

RU values observed in the absence of tPA (Fig. 5*A*), suggesting that the initial binding reflects the tPA-independent interaction of Mini-Pg with Fn. The secondary slow binding, which is only evident in the presence of FPR-tPA, results in a 1.5 ± 0.1-fold increase in total binding with all concentrations of Mini-Pg. This binding pattern is similar to the slow binding of FPR-tPA to Fn alone (Fig. 5*B*, *inset*), thus suggesting that this additional binding is tPA-dependent and that the binding characteristics of the Mini-Pg/Fn interaction are altered in the presence of tPA. Furthermore, the dissociation profiles in the presence of FPR-tPA are different from those observed in its absence and exhibit a slower rate of dissociation, suggesting that the Mini-Pg/Fn interaction is stabilized in the presence of FPR-tPA. In contrast to Mini-Pg, there was no measurable binding of Micro-Pg to Fn in the absence or presence of FPR-tPA (data not shown).

DISCUSSION

Fn and, to a lesser extent, Fg serve as cofactors that promote Pg activation by tPA. To exert this cofactor activity, Fn provides a template onto which tPA and Pg assemble (4, 5). Such assembly not only concentrates the reactants in close proximity, but may also induce conformational changes that promote their interaction. The importance of the interaction between tPA and Fn is highlighted by the fact that Fn cofactor activity is lost with uPA, a Pg activator that does not bind to Fn. However, the contribution of the Pg/cofactor interaction to the cofactor activity of Fn or Fg is less clear. To address this gap in knowledge, we used a series of Pg variants to examine the impact of Pg truncation on (*a*) Fn and Fg affinity, and (*b*) kinetics of activation by tPA or uPA in the absence or presence of Fg or Fn.

Removal of selected domains from Pg had predictable effects on affinity for Fn. Lys-Pg has higher affinity for Fn than Glu-Pg because its open conformation renders the lysine-binding kringle domains more accessible to Fn (26). Likewise, removal of most or all of the kringle domains progressively reduces the affinities of Mini- and Micro-Pg for Fn and Fg. Our binding data, which were obtained using SPR, complement previously reported results using Fn clots. With SPR, we were not only able to determine affinities of the Pg variants for Fn, but we also were able to compare affinities for Fn with those for Fg. Having verified the production of a panel of Pg variants with varying affinities for Fn and Fg, we next studied the kinetic of their activation by tPA in the absence or presence of Fn or Fg.

Because the Pg variants had different rates of activation, cofactor ratios were used to compare the influence of Fn or Fg on their catalytic efficiencies of activation. Despite the fact that Lys-Pg binds Fn with an affinity 2 orders of magnitude higher than that of Glu- or Mini-Pg, cofactor ratios with Glu-, Lys-, and Mini-Pg are similar. These results suggest that the substrate/cofactor interaction is not the primary determinant of the stimulatory effect of Fn or Fg. This concept is supported by the results with uPA; neither Fn nor Fg has a stimulatory effect on activation by uPA, which does not bind to Fn. Therefore, the cofactor activity of Fn or Fg is dependent on the tPA/Fn or tPA/Fg interaction; a concept supported by the Pg ratios that are higher for Lys-Pg or Mini-Pg than for Glu-Pg, regardless of whether the cofactor is Fn or Fg. These results point to the

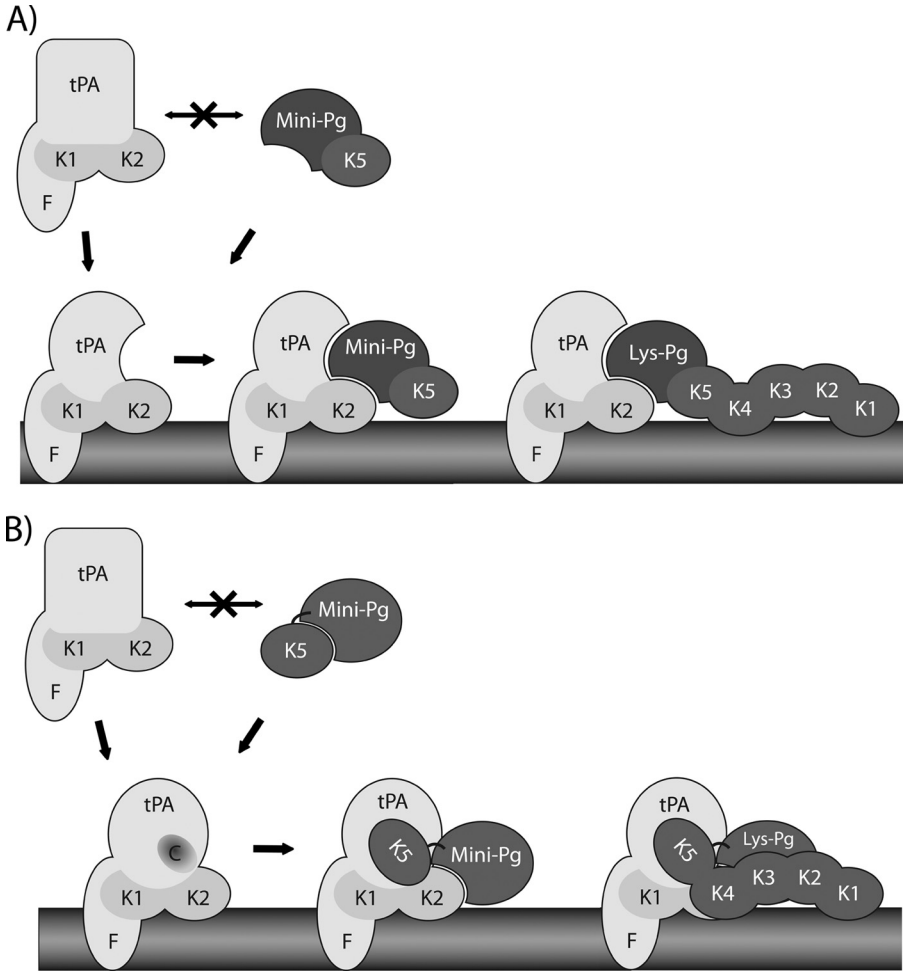

FIGURE 6. **Models of the interaction of Mini- or Lys-Pg with the tPA-Fn complex.** In the absence of Fn, neither Mini-Pg nor Lys-Pg interacts efficiently with tPA. *A,* the kringle 5 domain (*K5*) of Mini-Pg weakly binds Fn and localizes Mini-Pg in the vicinity of Fn-bound tPA. The interaction of tPA with Fn, which is primarily mediated by its finger (*F*) domain, induces conformational changes in tPA that enable an interaction between the kringle 2 domain (*K2*) of tPA and the protease domain of Pg. *B*, the interaction of tPA with Fn exposes a cryptic binding site on tPA (designated *C*) that interacts with the K5 domain of Mini-Pg. This interaction facilitates the interaction of the protease domain of Mini-Pg with the K2 domain of tPA. The interaction of Lys-Pg with the tPA-Fn complex is similar to that of Mini-Pg, except kringle domains 1 and 4 also help anchor Lys-Pg to Fn.

tPA/Fn interaction as the primary determinant of cofactor activity.

By studying Micro-Pg, which lacks kringle domains, we were able to further examine the contribution of the substrate/cofactor interaction to cofactor activity. Because it only possesses the protease domain, Micro-Pg should be at least as readily activable as Lys- and Mini-Pg. However, Fn and Fg have minimal effects on the catalytic efficiency of its activation by tPA. In contrast, Fn enhances the catalytic efficiency of Mini-Pg activation by tPA, even though the affinity of Mini-Pg for Fn is very low. The presence of the kringle 5 domain distinguishes Mini-Pg from Micro-Pg. Therefore, the absence of a kringle 5 domain limits Micro-Pg activation by Fn-bound tPA, which raises the possibility that this domain, and possibly the other kringle domains, play a part in Pg activation that extends beyond Fn binding and involves direct interaction with Fn-bound tPA.

Because the tPA/cofactor interaction is critical for expression of cofactor activity, we used SPR to explore the possibility that tPA influences the interaction of Pg with Fn. Compared with injection of Mini-Pg alone, co-injection of FPR-tPA and Mini-Pg enhances Fn binding and increases the stability of the ternary complex, as evidenced by the slower off-rate (Fig. 5*B*). These observations support the hypothesis proposed by Horrevoets *et al.* (4) that the stability of the ternary complex is a more important determinant of the catalytic efficiency of Pg activation than the affinity of the enzyme or the substrate for Fn. What remains uncertain is the exact mechanism by which the tPA/Pg interaction stabilizes the ternary complex.

Our data identify at least two mechanisms by which formation of the ternary tPA-Pg-Fn complex enhances Pg activation. First, the interaction between tPA and Mini-Pg is altered when they are localized on the Fn surface (Fig. 6*A*). tPA binds to Fn predominantly via its finger domain, whereas the kringle 5 domain of Mini-Pg mediates only a weak interaction with Fn. The conformational change that occurs when tPA binds to Fn (27, 28) may promote an interaction between its kringle 2 domain and the protease domain of Pg. The closed conformation of Glu-Pg and kringles 1 through 4 on Lys-Pg likely render the tPA binding site on the protease domain of Pg less accessible, thereby explaining why Glu-Pg exhibits little or no binding to tPA and Micro-Pg binds tPA with higher affinity than either Mini-Pg or Lys-Pg (Fig. 3).

Alternatively, tPA binding to Fn may expose a cryptic binding site on tPA that is specific for the kringle 5 domain of Pg (Fig. 6*B*). Binding of the kringle 5 domain to the tPA-Fn complex may not only anchor Pg within the ternary complex, but may also better position the substrate for tPA-mediated activation. Binding of Mini-Pg to Fn is increased in the presence of FPR-tPA (Fig. 5*B*). Although this may reflect increased binding of Mini-Pg and/or tPA to Fn, the slow association of this interaction is similar to that observed when FPR-tPA binds to Fn (Fig. 5*B*, *inset*), where the plateau is only reached after 30 s. By comparison, the association of Mini-Pg with Fn (Fig. 5*A*) or with tPA (data not shown) rapidly reaches a plateau. Taken together, it is likely that Mini-Pg and tPA bind to distinct sites on the Fn surface, and that the additional binding observed when the two are co-injected reflects an interaction of Mini-Pg with the tPA-Fn complex, which is distinct from its interaction with Fn alone. Accordingly, the formation of the initial tPA-Fn complex is the rate-limiting step, which explains why the binding profile resembles that of the tPA/Fn interaction (Fig. 5*B*, *inset*). Thus, we hypothesize that the kringle 5 domain of Pg plays a unique role in Pg activation that extends beyond Fn binding. This explains why Fn and Fg potentiate the activation of Mini-Pg by tPA to a similar extent as they do Glu-Pg and Lys-Pg, even though kringle 5 is less important for Fn binding than kringles 1 and 4 (23, 24, 29).

Based on kinetic analyses, other researchers have proposed sequential or parallel models for assembly of the ternary Pg activation complex (4, 5). In the sequential model, Fn binds tPA prior to Pg, whereas in the parallel assembly model, Pg and tPA bind Fn in random order. The parallel model accommodates the apparent Fn concentration dependence of the k_{cat} at Fn concentrations below 1 μM (4). Because these conditions were not examined here, the significance of this aspect of the parallel assembly model is unclear. Our data are consistent with initial tPA binding to Fn to generate a binary enzymatic complex, as suggested by Hoylaerts *et al.* (5). Further support for the sequential assembly model comes from the fact that formation of binary Pg-Fn or Pg-tPA complexes is likely to be negligible *in vivo* because of the high K_d values.

In summary, our data suggest a novel role for the kringle 5 domain of Pg in efficient Pg activation by the tPA-Fn complex. This may represent a key regulatory step in Pg activation that provides a unique target for controlling Pn generation.

REFERENCES

1. Lijnen, H. R., and Collen, D. (1995) *Hematology. Basic Principles and Practice*, Churchill Livingstone, New York
2. Bachmann, F. (1994) *Hemostasis and Thrombosis: Basic Principles and Clinical Practice*, J. B. Lipincott Co., Philadelphia, PA
3. Fredenburgh, J. C., and Nesheim, M. E. (1992) Lys-plasminogen is a significant intermediate in the activation of Glu-plasminogen during fibrinolysis *in vitro*. *J. Biol. Chem.* **267,** 26150–26156
4. Horrevoets, A. J., Pannekoek, H., and Nesheim, M. E. (1997) A steady-state template model that describes the kinetics of fibrin-stimulated [Glu[1]]- and [Lys[78]]plasminogen activation by native tissue-type plasminogen activator and variants that lack either the finger or kringle-2 domain. *J. Biol. Chem.* **272,** 2183–2191
5. Hoylaerts, M., Rijken, D. C., Lijnen, H. R., and Collen, D. (1982) Kinetics of the activation of plasminogen by human tissue plasminogen activator. Role of fibrin. *J. Biol. Chem.* **257,** 2912–2919
6. Bachmann, F. (2001) *Hemostasis and Thrombosis*, Lippincott Williams & Wilkins, Philadelphia, PA
7. Lijnen, H. R., Bachmann, F., Collen, D., Ellis, V., Pannekoek, H., Rijken, D. C., and Thorsen, S. (1994) Mechanisms of plasminogen activation. *J. Intern. Med.* **236,** 415–424
8. Collen, D., and Lijnen, H. R. (1991) Basic and clinical aspects of fibrinolysis and thrombolysis. *Blood* **78,** 3114–3124
9. Sottrup-Jensen, L., Claeys, H., Zajdel, M., Petersen, T. E., and Magnusson, S. (1978) *Progress in Chemical Fibrinolysis and Thrombolysis*, Raven Press, New York, NY
10. Castellino, F. J., Ploplis, V. A., Powell, J. R., and Strickland, D. K. (1981) The existence of independent domain structures in human Lys[77]-plasminogen. *J. Biol. Chem.* **256,** 4778–4782
11. Straughn, W., 3rd, and Wagner, R. H. (1966) A simple method for preparing fibrinogen. *Thromb. Diath. Haemorrh.* **16,** 198–206
12. Walker, J. B., and Nesheim, M. E. (1999) The molecular weights, mass distribution, chain composition, and structure of soluble fibrin degradation products released from a fibrin clot perfused with plasmin. *J. Biol. Chem.* **274,** 5201–5212
13. Castellino, F. J., and Powell, J. R. (1981) Human plasminogen. *Methods Enzymol.* **80,** 365–378
14. Stewart, R. J., Fredenburgh, J. C., and Weitz, J. I. (1998) Characterization of the interactions of plasminogen and tissue and vampire bat plasminogen activators with fibrinogen, fibrin, and the complex of D-dimer noncovalently linked to fragment E. *J. Biol. Chem.* **273,** 18292–18299
15. Nesheim, M., Fredenburgh, J. C., and Larsen, G. R. (1990) The dissociation constants and stoichiometries of the interactions of Lys-plasminogen and chloromethyl ketone derivatives of tissue plasminogen activator and the variant delta FEIX with intact fibrin. *J. Biol. Chem.* **265,** 21541–21548
16. Wu, H. L., Chang, B. I., Wu, D. H., Chang, L. C., Gong, C. C., Lou, K. L., and Shi, G. Y. (1990) Interaction of plasminogen and fibrin in plasminogen activation. *J. Biol. Chem.* **265,** 19658–19664
17. Shi, G. Y., and Wu, H. L. (1988) Isolation and characterization of microplasminogen. A low molecular weight form of plasminogen. *J. Biol. Chem.* **263,** 17071–17075
18. Fredenburgh, J. C., Stafford, A. R., Leslie, B. A., and Weitz, J. I. (2008) Bivalent binding to γA/γ′-fibrin engages both exosites of thrombin and protects it from inhibition by the antithrombin-heparin complex. *J. Biol. Chem.* **283,** 2470–2477
19. Vu, T. T., Stafford, A. R., Leslie, B. A., Kim, P. Y., Fredenburgh, J. C., and Weitz, J. I. (2011) Histidine-rich glycoprotein binds fibrin(ogen) with high affinity and competes with thrombin for binding to the γ′-chain. *J. Biol. Chem.* **286,** 30314–30323
20. Senis, Y. A., Kim, P. Y., Fuller, G. L., García, A., Prabhakar, S., Wilkinson, M. C., Brittan, H., Zitzmann, N., Wait, R., Warrell, D. A., Watson, S. P., Kamiguti, A. S., Theakston, R. D., Nesheim, M. E., and Laing, G. D. (2006) Isolation and characterization of cotiaractivase, a novel low molecular weight prothrombin activator from the venom of *Bothrops cotiara*. *Biochim. Biophys. Acta* **1764,** 863–871
21. Schneider, M., and Nesheim, M. (2004) A study of the protection of plasmin from antiplasmin inhibition within an intact fibrin clot during the course of clot lysis. *J. Biol. Chem.* **279,** 13333–13339
22. Lucas, M. A., Fretto, L. J., and McKee, P. A. (1983) The binding of human plasminogen to fibrin and fibrinogen. *J. Biol. Chem.* **258,** 4249–4256
23. Motta, A., Laursen, R. A., Llinás, M., Tulinsky, A., and Park, C. H. (1987) Complete assignment of the aromatic proton magnetic resonance spectrum of the kringle 1 domain from human plasminogen. Structure of the ligand-binding site. *Biochemistry* **26,** 3827–3836
24. Petros, A. M., Ramesh, V., and Llinás, M. (1989) ^{1}H NMR studies of aliphatic ligand binding to human plasminogen kringle 4. *Biochemistry* **28,** 1368–1376
25. Lin, X., Takahashi, K., Campion, S. L., Liu, Y., Gustavsen, G. G., Peña, L. A., and Zamora, P. O. (2006) Synthetic peptide F2A4-K-NS mimics fibroblast growth factor-2 in vitro and is angiogenic *in vivo*. *Int. J. Mol. Med.* **17,** 833–839
26. Suenson, E., and Thorsen, S. (1988) The course and prerequisites of Lys-plasminogen formation during fibrinolysis. *Biochemistry* **27,** 2435–2443

27. Lamba, D., Bauer, M., Huber, R., Fischer, S., Rudolph, R., Kohnert, U., and Bode, W. (1996) The 2.3-Å crystal structure of the catalytic domain of recombinant two-chain human tissue-type plasminogen activator. *J. Mol. Biol.* **258,** 117–135
28. Renatus, M., Bode, W., Huber, R., Stürzebecher, J., Prasa, D., Fischer, S., Kohnert, U., and Stubbs, M. T. (1997) Structural mapping of the active site specificity determinants of human tissue-type plasminogen activator. Implications for the design of low molecular weight substrates and inhibitors. *J. Biol. Chem.* **272,** 21713–21719
29. Thewes, T., Constantine, K., Byeon, I. J., and Llinás, M. (1990) Ligand interactions with the kringle 5 domain of plasminogen. A study by ^{1}H NMR spectroscopy. *J. Biol. Chem.* **265,** 3906–3915
30. Dobrovolsky, A. B., and Titaeva, E. V. (2002) The fibrinolysis system. Regulation of activity and physiologic functions of its main components. *Biochemistry* **67,** 99–108
31. Komorowicz, E., Kolev, K., and Machovich, R. (1998) Fibrinolysis with des-kringle derivatives of plasmin and its modulation by plasma protease inhibitors. *Biochemistry* **37,** 9112–9118
32. Horrevoets, A. J., Smilde, A. E., Fredenburgh, J. C., Pannekoek, H., and Nesheim, M. E. (1995) The activation-resistant conformation of recombinant human plasminogen is stabilized by basic residues in the amino-terminal hinge region. *J. Biol. Chem.* **270,** 15770–15776
33. Lijnen, H. R. (2001) Elements of the fibrinolytic system. *Ann. N.Y. Acad. Sci.* **936,** 226–236